Mechanical and thermal properties of hybrid nanocomposites prepared by *in situ* polymerization

Sandra Paszkiewicz[1), *)], Iwona Pawelec[2)], Anna Szymczyk[2)], Zbigniew Rosłaniec[1)]

DOI: dx.doi.org/10.14314/polimery.2016.172

Abstract: Poly(trimethylene terephthalate) (PTT) nanocomposites containing carbon nanoadditives which differ in shape (1D, 2D) and particle size were synthesized by *in situ* polymerization method. SEM and TEM images showed that expanded graphite (EG) and single-walled carbon nanotubes (SWCNTs) were well dispersed in PTT, suggesting that *in situ* polymerization is a highly efficient method for preparing nanocomposites. Synergistic effect between single-walled carbon nanotubes and expanded graphite on improving mechanical and thermal properties of the prepared nanocomposites has been observed.

Keywords: single-walled carbon nanotubes, expanded graphite, polymer hybrid nanocomposites, *in situ* polymerization, mechanical properties, thermal stability.

Właściwości mechaniczne i termiczne hybrydowych nanokompozytów polimerowych otrzymanych metodą polimeryzacji *in situ*

Streszczenie: Metodą polimeryzacji *in situ* zsyntetyzowano nanokompozyty na bazie poli(tereftalanu trimetylenu) (PTT) zawierające nanododatki węglowe [jednościenne nanorurki węglowe (SWCNTs) i grafit ekspandowany (EG)] różniące się kształtem (1D, 2D) i wielkością cząstek. Badania metodami SEM i TEM wykazały, że nanowarstwy grafitu i nanorurki są dobrze zdyspergowane w PTT, co sugeruje, że polimeryzacja *in situ* jest bardzo skuteczną metodą wytwarzania nanokompozytów. Zaobserwowano synergiczny wpływ nanorurek węglowych i ekspandowanego grafitu na poprawę właściwości mechanicznych i termicznych otrzymanych nanokompozytów.

Słowa kluczowe: jednościenne nanorurki węglowe, ekspandowany grafit, hybrydowe nanokompozyty polimerowe, polimeryzacja *in situ*, właściwości mechaniczne, stabilność termiczna.

Poly(trimethylene terephthalate) (PTT) is a relatively new semicrystalline polymeric material developed by Shell Chemical Company [1, 2]. It can be characterized by a high strength and resistance to high temperatures. Unlike all other known linear polyester polymers, PTT fibres show a repeatable elastic recovery of about 10—12 %. With a better resilience and elastic recovery if compared to PET and PBT, PTT can replace them in many applications [3, 4]. Carbon-based nanomaterials such as carbon nanotubes (1D) and expanded graphite (2D) are well-known for their extremely high mechanical properties, electrical and thermal conductivity and relatively low density [5]. They are extensively considered as perfect fillers for polymers due to improving their mechanical, thermal and electrical properties. They can be used in the fabrication of multifunctional polymer composites [6, 7]. Carbon nanotubes (CNT) have been described as rolled-up graphene layers. Single-walled carbon nanotubes (SWCNTs) have been extensively studied as a typical one-dimensional system due to their unique electrical, chemical, optical, and mechanical properties. Depending on their structural parameters, SWCNTs can be metallic or semiconducting [8, 9]. One should also pay attention to the special properties of graphene. The main advantages of graphene including exceptional thermal conductivity (5000 $W \cdot m^{-1} K^{-1}$), mechanical properties with Young's modulus of 1 TPa and ultimate strength of 130 GPa [10—12]. Furthermore, graphene has an extremely high surface area and gas impermeability, thus has great potential for improving electrical, mechanical, thermal and gas barrier properties of polymers [6, 7]. In addition to above mentioned advantages, the nanocomposites possess some drawbacks which include high price, difficulty in obtaining high and uniform level of dispersion in the polymer and nanofiller's tendency to agglomerate.

Interesting from the point of view of their impact of the electrical and mechanical properties seems to be the introduction of two types of carbon nanofillers such as EG and CNT to the polymer matrix. The synergistic effect created with respect to the addition of two different car-

[1)] West Pomeranian University of Technology, Institute of Material Science and Engineering, Piastow Av. 19, 70-310 Szczecin, Poland.

[2)] West Pomeranian University of Technology, Institute of Physics, Piastow Av. 19, 70-310 Szczecin, Poland.

[*)]Author for correspondence; e-mail: spaszkiewicz@zut.edu.pl

bon nanostructures, may be a result of excellent dispersion of nanofillers in the polymer matrix due to their unique geometric structures. It might be also a result of the formation of conducting network in the polymer. It has been already observed, that a remarkable synergistic effect between the SWCNT and EG can improve the mechanical properties and thermal conductivity of polyester nanocomposites [13].

The aim of our study was to develop innovative electrically conductive polymer hybrid nanocomposites with the lowest possible content of EG and SWCNTs, with a balanced mechanical and thermal properties. In our previous studies nanocomposites based on PET [12, 14—16] and PTT/PTMO [9, 17, 18] with single-walled carbon nanotubes and expanded graphite (or other graphene derivative form) were investigated. Therefore, it seems to be interesting to investigate the effect of nanofillers on the thermal and mechanical properties of PTT based hybrid nanocomposites. For this purpose, composites based on PTT with SWCNTs, EG and the mixture of both were prepared.

This article is only a part of the wider project on the possibility of obtaining electrically conductive polymer hybrid nanocomposites containing carbon nanoparticles such as EG and SWCNTs. Therefore, in the present study the effect of the CNT-GNP (carbon nanotubes-graphene nanoplatelets) on the morphology, thermal and mechanical properties as well as thermal stability with a total content not exceeding 0.2 wt % of nanofillers in the polymer matrix has been investigated. Such a low content of carbon nanoparticles, *i.e*. SWCNTs and EG is justified by their high cost. Moreover, our previous studies on electrically conductive polymer nanocomposites based on PET with SWCNTs [19] or EG [16] demonstrated percolation threshold as low as 0.05 wt %.

EXPERIMENTAL PART

Materials

For neat PTT and PTT based nanocomposites' synthesis the following substrates were used in this study: dimethyl terephthalate (DMT) (Sigma - Aldrich); bio-1,3-propanediol (PDO) (Susterra® Propanediol, DuPont Tate & Lyle, USA), as catalysts: the tetrabutyl orthotitanate [$Ti(OBu)_4$, Fluka] and as an antioxidant the tetrakis[methylene(3,5-di-butyl-4-hydroxyphenyl-hydro-cinnamate)]methane (Irganox 1010, Ciba-Geigy, Basel, Switzerland).

The single-walled carbon nanotubes KNT 95 (SWCNTs) were purchased from Grafen Chemical Industries (Grafen Co.) with the suppliers data sheet: diameter < 2 nm, electrical conductivity > 100 S/cm, length 5—30 μm, purity > 95 %, surface area 380 m^2/g. Expanded graphite was provided by Polymer Institute of Slovak Academy of Science with platelets size of around 50 μm. XPS analysis provide following information: C1s 99.21 % and O1s 0.79 %.

Preparation of PTT/SWCNTs + EG nanocomposites

Nanocomposites with SWCNTs and expanded graphite were prepared by *in situ* polymerization. Nanocomposites were prepared by *in situ* polymerization using 1 dm^3 polycondensation reactor (Autoclave Engineering Inc., USA). Before polymerization, the SWCNTs and/or EG were dispersed in PDO using high-speed stirrer (Ultra-Turrax® T25) and ultrasonic homogenizer (Sonoplus HD 2200, Bandelin) for 30 min. Additionally, to improve the dispersion/exfoliation of EG in PDO an ultra-power lower sonic bath was applied for 8 hours. The polymerization process was conducted in two stages. In the first stage, a transesterification reaction took place between dimethyl terephthalate (DMT) and 1,3-propanediol under nitrogen flow at atmospheric pressure and in a temperature range of 160—180 °C. The methanol formed during the transestrification was distilled off and collected. The second stage was begun when the pressure was gradually lowered to about 20 Pa and the polycondensation was carried out at temperature of 260 °C and under continuous stirring. The progress of the polymerization was monitored by measuring the changes of viscosity of the polymerization mixture, *i.e*. an increase in torque stirrer values during the polycondensation. The reaction was considered complete when the viscosity of the system increased to 14 Pa·s. The obtained polymer/nanocomposite was extruded from the reactor under nitrogen flow in the form of polymer wire.

Samples preparation

Dumbbell shape samples (ISO 37 type 3) of nanocomposites for SEM, tensile and density tests were obtained by injection molding at a pressure of around 50 MPa and at temperature of 250 °C and injected into the injection molding form heated to the temperature of 30 °C. Due to the high sensitivity to moisture of PTT during processing, before injection molding all samples were dried for 24 h under vacuum.

Methods of testing

— The structure of the nanocomposites was observed using scanning electron microscope (SEM, JEOL JSM 6100). The sample for the testing were cryo-fractured in liquid nitrogen and then vacuum coated with a thin gold film. Transmission electron microscopy (TEM) analysis was carried out by a PHILLIPS CM 120 Electron Microscope using an acceleration voltage of 80 kV. In the case of TEM examination the specimens were cut from the central part of the dumbbell shaped sample using Reichert Ultracut R ultramicrotome with a diamond knife.

— The intrinsic viscosity [η] of the polymer/nanocomposites samples was determined at 30 °C in the mixture of phenol/1,1,2,2-tetrachloroethane (60/40 by weight) accordingly to the procedure presented elsewhere [4, 12,

14—18]. Through Mark-Houwink equation, that relates the limiting viscosity number with molecular weight, the viscosity average molecular weight (M_v) has been calculated using formula 1:

$$[\eta] = K \cdot M_v^{\alpha} \quad (1)$$

where: K, α — constants specific to the solvent and temperature. The viscosity average molecular weight (M_v) of neat PTT and its composites was calculated using following constants: $K = 5.36 \cdot 10^{-2}$ cm^3/g and $\alpha = 0.69$ [20].

— Density measurement (d) was conducted on the injection moulded dumbbell shape samples using a hydrostatic scales (Radwag WPE 600C, Poland), calibrated using standards with known density. Additionally, weight degree of crystallinity (X_{cw}) was quantified based on the density measurements using the Formula (2):

$$X_{cw} = \frac{\rho_c}{\rho} \frac{(\rho - \rho_a)}{(\rho_c - \rho_a)} \cdot 100\ \% \quad (2)$$

where: ρ — measured density of semicrystalline sample, ρ_a — density if the sample is completely amorphous, ρ_c — density if the sample is completely crystalline. For neat PTT and its composites: $\rho_a = 1.299$ g/cm^3, $\rho_c = 1.432$ g/cm^3 [21].

— Differential scanning calorimetry (DSC) measurements were carried (TA, Q100) under a nitrogen atmosphere in a temperature range from 25 to 300 °C and sample weight of 10 ± 0.2 mg. Each DSC test comprised of the heating-cooling-heating cycle at the heating-cooling rate of 10 °C/min. The glass transition temperature (T_g) of the polymer samples was taken as the midpoint of the change in heat capacity from the second heating scan. The first cooling and second heating scans were used to determine the melting and crystallization peaks. The degree of crystallinity of the sample (X_c) was calculated using the same procedure as described in [12, 14—18] using Formula (3):

$$X_c = \frac{\Delta H_m}{\Delta H_m^0} \cdot 100\ \% \quad (3)$$

where: ΔH_m^0 — the enthalpy change of melting for a 100 % crystalline sample (for PTT: $\Delta H_m^0 = 146$ J/g [21] and ΔH_m is derived from melting peak area on DSC thermograms).

— Thermal and thermo-oxidative stability of investigated polymer nanocomposites were evaluated by thermogravimetry (TGA 92-16.18 Setaram). Measurements were carried out in an inert (argon) and in oxidizing atmosphere *i.e.* dry, synthetic air (N_2 : O_2 = 80 : 20 vol %). The study was conducted in the temperature range from 20 to 600 °C at a heating rate of 10 °C/min. Measurements were performed in accordance to the standard PN-EN ISO 11358:2004.

— Tensile measurements were performed using Instron 5566 universal tensile testing frame, equipped with a 5 kN Instron load cell, a contact optical long travel extensometer and the Bluehill 2 software. The measurements were performed at room temperature on using a cross-head speed of 5 mm/min and a grip distance of 20 mm. The Young's modulus, yield stress (elastic limit), yield strain, yield stress and elongation at break of the nanocomposites were determined. The E modulus is defined as the tangent of the slope angle of a stress – strain curve in the linear relation and determined in accordance with ASTM E111-04 (2010). The results are based on data collected from 6 specimens for each sample and the mean values and standard deviations were calculated.

RESULTS AND DISCUSSION

Physical properties of PTT/SWCNTs + EG hybrid nanocomposites

Table 1 presents the intrinsic viscosity and density of PTT based nanocomposites with SWCNTs, EG and with hybrid mixture of both nanofillers. For PTT/EG nanocomposites the decrease in [η] was observed. On the other hand, the addition of SWCNTs to PTT matrix caused increase in [η], and thus causing an increase in molecular mass. There was no significant effect of the addition of carbon nanoparticles on the molecular masses of the prepared nanocomposites which were within the range of 38 100 and 39 600 g/mol and they were comparable to the molecular mass obtained for neat PTT *i.e.* 38 400 g/mol. In both cases, it was observed that carbon nanotubes determined both morphology and mechanical properties, without apparent effect of agglomerates of EG.

T a b l e 1. Physical properties of PTT/SWCNTs + EG nanocomposites

Sample	[η] cm^3/g	$M_v \cdot 10^4$ g/mol	d g/cm^3	X_{cw} %
PTT	78.1	3.84	1.323	19.8
PTT/0.1 EG	77.7	3.81	1.328	23.4
PTT/0.05 SWCNTs + 0.1 EG	78.2	3.85	1.322	18.9
PTT/0.1 SWCNTs + 0.1 EG	78.9	3.90	1.313	12.2
PTT/0.05 SWCNTs	79.8	3.96	1.329	24.6
PTT/0.1 SWCNTs	78.4	3.85	1.324	20.6

M_v — viscosity average molecular mass, d — density; X_{cw} — weight degree of crystallinity estimated from density measurement.

On the other hand, the density for both hybrid nanocomposites decreased with the increasing content of SWCNTs. At the same time the weight degree of crystallinity strongly decreased if compared to neat PTT but also to both „single" nanocomposites. These results indicated that the incorporation of appropriate amount of SWCNTs/EG nanoparticles had strong effect on the degree of crystallinity of PTT. The effect of the presence of SWCNTs on non-isothermal crystallization behavior of PTT nanocomposites observed here, is in contrast to the results reported in literature for PTT composites containing MWCNTs [4], where the presence of MWCNTs decrease crystallization rate of PTT in composites.

Dispersion of EG and SWCNTs in PTT based hybrid nanocomposites

SEM and TEM were used to visually evaluate the degree of exfoliation and the amount of aggregation of nanofillers in poly(trimethylene terephthalate) matrix. TEM analysis tends to support the findings from SEM but also shows that the SWCNTs nanoparticles were well dispersed on the nanoscale in all systems.

SEM analysis of the fracture surfaces of PTT/SWCNTs nanocomposites indicates rather homogenous distribution of carbon nanotubes in the PTT matrix. In the case of prepared composites in the observed TEM micrographs some nanoinclusions can be distinguished that are uniformly distributed in the polymer with small agglomerate.

To confirm the morphological features of EG in the PTT matrix, SEM images of the fractured surfaces for the

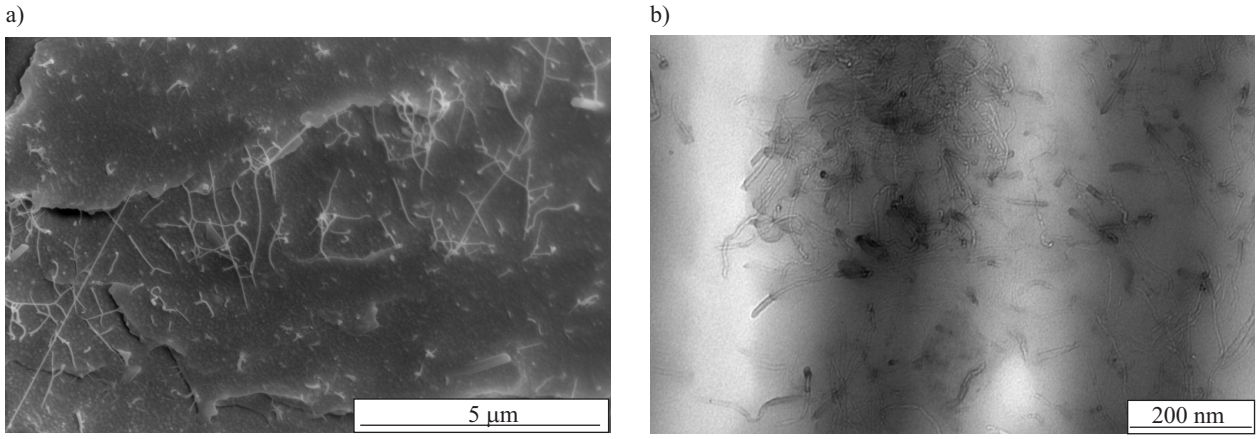

Fig. 1. a) TEM (x 200.000), b) SEM images of PTT/0.1 SWCNTs nanocomposites

Figure 1a shows SEM micrographs of fracture surfaces of PTT nanocomposites with nanotubes. As is generally known, that CNTs often tend to bundle together by van der Waals interaction between the individual nanotubes with high aspect ratio and large surface area and lead to some agglomerations, which prevent efficient load transfer from matrix to nanotube. Moreover, most of the nanotubes show pulling out and sliding at the surface of nanocomposite, suggesting a limitation of load transfer to nanotube. Individual nanotubes with some entanglements or bundles of CNT, apparently pulled out from the matrix during fracturing are observed on the surface. nanocomposite films were examined, as can be seen in Fig. 2a. For further investigation, the TEM analysis was used to assess the degree of exfoliation of the expanded graphite platelets and the morphology of the nanocomposites (Fig. 2b). From this micrograph, more or less transparent graphene platelets has been observed, which confirmed a high degree of exfoliation of EG in a matrix. The fractured surface of PTT/EG composite film with 0.1 wt % EG also exhibits the smooth fractured surface without exhibiting any aggregates of graphene sheets. Nonetheless, it should be mentioned that the partial aggregates of graphene sheets in the nanocomposites

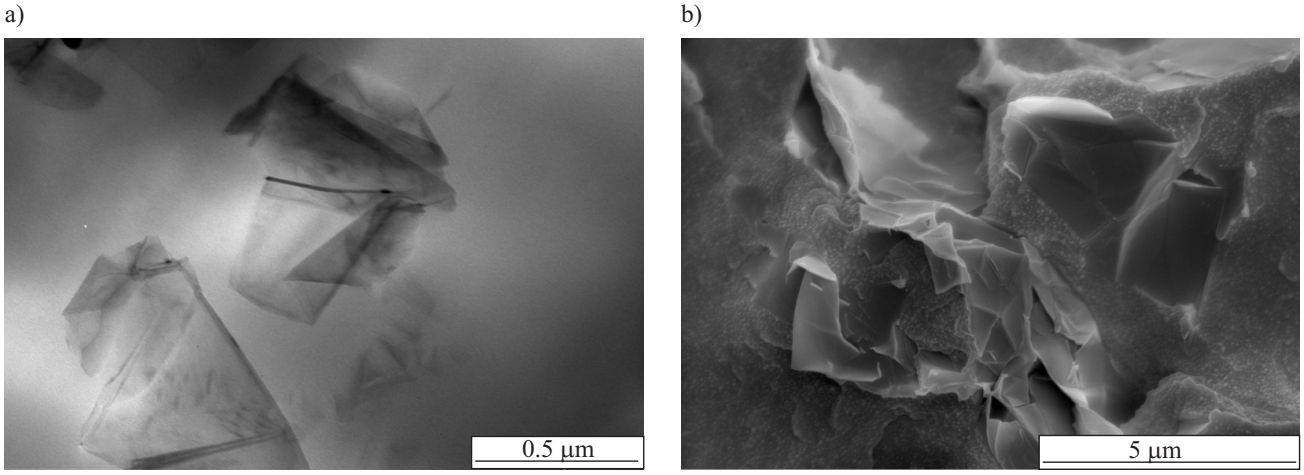

Fig. 2. a) TEM (x 100.000), b) SEM images of PTT/0.1 EG nanocomposites

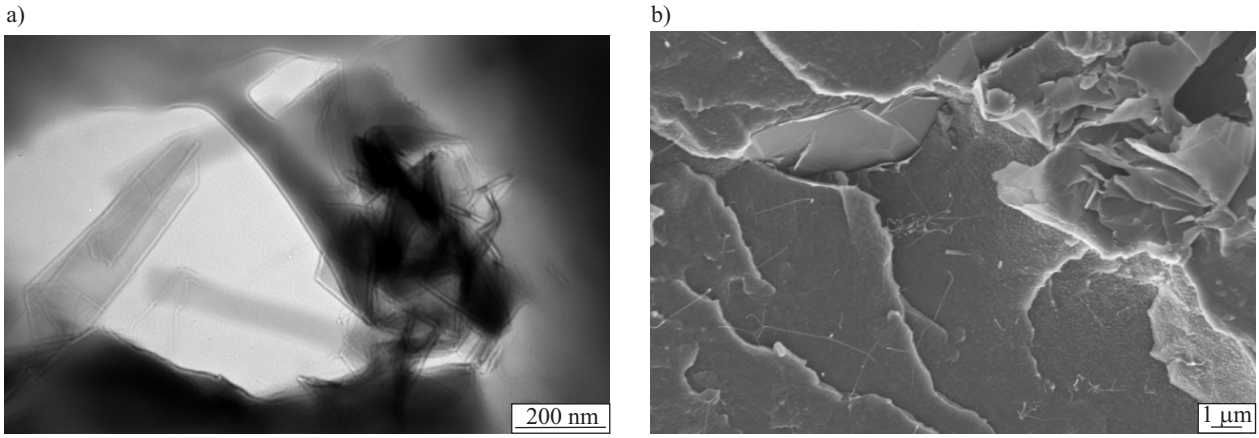

Fig. 3. a) TEM (x 150.000), b) SEM images of PTT/0.05 SWCNTs + 0.1 EG nanocomposites

(Fig. 2a) with higher EG contents are not crystalline forms but disordered structure, as confirmed from density and DSC measurements. In addition, the accordion-like structures detected in the PTT/EG nanocomposites means that the expanded graphite sheets exist in a completely exfoliated and disordered state in the matrix due to the high shear force generated during dispersion preparation followed by *in situ* polymerization. Direct evidence of the exfoliation of expanded graphite was provided by TEM analysis of PTT/0.1EG nanocomposites. The exfoliated structure with clearly visible flakes (partially transparent) was observed. The flakes size was around 0.5x1 (μm^2), which was probably due to the *in situ* procedure and dispersion process before polymerization, that causes wrapping and breaking of graphene sheets. It was observed that the expanded graphite sheets were dispersed homogeneously in PTT matrix. The occurrence of this exfoliation structure may be attributed to the strong shear field in the mechanical stirrer and treatment of ultrasounds, and the strong interactions between EG and PTT.

The efficiency of the hybrid system in modifying the properties of the matrix polymer is primarily determined by the degree of its dispersion in the polymer matrix. The aggregated EG structure can be characterized with SEM. Because of the difference in scattering density between the nanofiller and PTT, nanoplatelets aggregates can be easily imaged in SEM. At the same time well-dispersed carbon nanotubes were clearly visible. More direct evidence of the formation of a structure of nanocomposite is provided by TEM from an ultramicrotomed section. Figure 3a shows micrograph of PTT hybrid containing 0.05 SWCNTs + 0.1 EG. The dark regions in the micrograph are thicker agglomerates of expanded graphite (less expanded), and the brighter regions show better dispersed sheets. TEM micrograph proves that some graphene layers were dispersed homogeneously in the matrix polymer, however mostly clusters or agglomerated particles were detected. This will be cross-checked by ultimate strength and initial modulus in the tensile property section.

Influence of the hybrid system SWCNTs + EG on the crystallization of PTT

Figure 4 show the DSC thermograms during cooling and 2nd heating of neat PTT and PTT/SWCNTs + EG hybrid nanocomposites. Furthermore, the glass transition temperature (T_g) data helps to understand the effects of hybrid system of particles on the movement of polymer chains. DSC showed no influence in the glass transition temperature (T_g) of the nanocomposite prepared by *in situ* polymerization as compared to neat polymer and nanocomposites with „single" nanofillers (Table 2). No influence in T_g is related to the nanocomposite morphology but also to its high molecular masses; PTT/0.1SWCNTs + 0.1 EG nanocomposite presented an average molecular mass of $3.9 \cdot 10^4$ versus $3.84 \cdot 10^4$ for neat PTT. Hybrid nanofillers didn't affect the chain mobility of PTT. It is evident that there was a distinct exothermic crystallization peak in all of the cooling scans and the peak is symmetrical. The DSC thermograms recorded during cooling of the samples from melt with a constant cooling rate showed a prominent crystallization exothermic peak. The results for PTT/SWCNTs + EG nanocomposites are listed in Table 2. The crystallization temperatures T_c and the ΔH_c values for PTT/SWCNTs + EG nanocomposites are higher than those of neat PTT. The PTT/0.1SWCNTs + 0.1 EG exhibited the highest T_c value (184 °C) form the whole series of the prepared nanocomposites. Changes in the crystallization peak width and the heat of crystallization (ΔH_c) are related to the overall crystallization rate and the extent of crystallization, respectively. The T_c peaks' width for both hybrid nanocomposites are narrower than that of neat PTT. On the other hand, the values of ΔH_c for hybrid nanocomposites are larger than that of PTT (36.2 J/g), however they decrease with increase in the SWCNTs content.

From these results, it can be concluded that 0.1 SWCNTs + 0.1 EG exhibits a strong heterophase nucleation effect on PTT crystallization due to its enormous surface area of both carbon nanofillers. The crystallization rate of PTT may be accelerated by the addition of

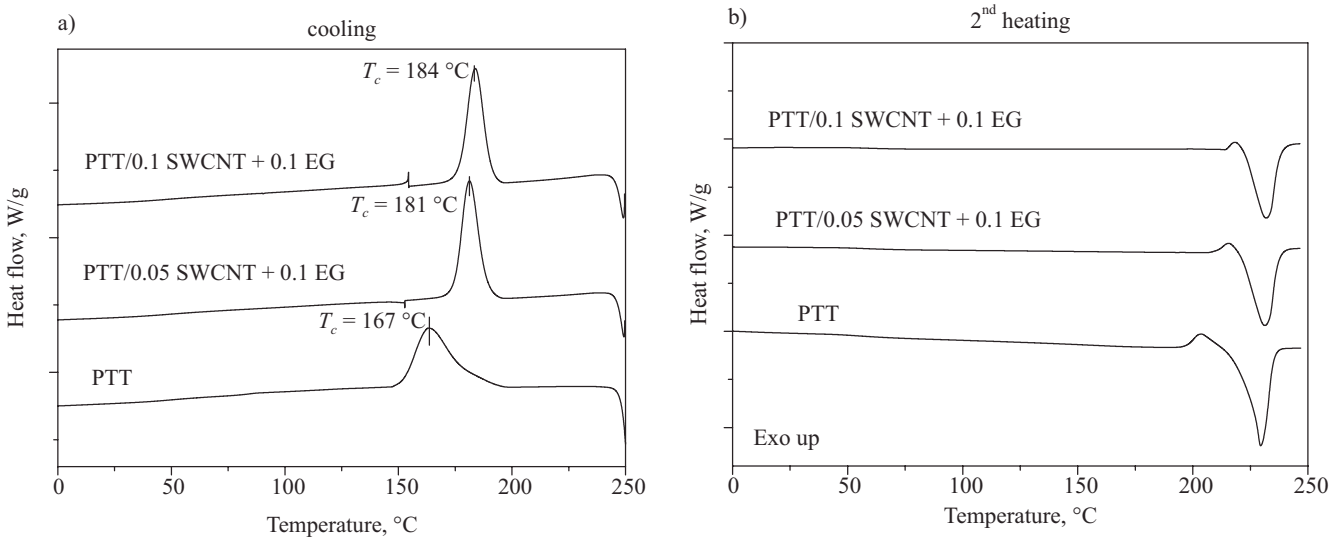

Fig. 4. DSC thermograms for PTT and PTT/SWCNTs + EG nanocomposites during the: a) cooling, b) 2nd heating

0.1 wt % of SWCNTs and 0.1 wt % of EG, where the acceleration efficiency probably reaches a maximum at this level. In both systems (0.05 + 0.1 and 0.1 + 0.1), EG together with SWCNTs is an effective nucleating agent due to the high surface area of graphene platelets and their chemical affinity for the polymer, which induce a nucleation and lamellar ordering effect.

T a b l e 2. The phase transition temperatures and the degree of crystallinity of neat PTT and PTT/SWCNTs + EG nanocomposites determined by DSC

Symbol	T_g °C	T_m °C	ΔH_m J/g	T_c °C	ΔH_c J/g	X_c %
PTT	53	231	45.8	167	36.2	31.4
PTT/0.1 EG	53	230	47.9	180	47.1	32.8
PTT/0.05 SWCNTs + 0.1 EG	53	231	48.7	181	47.9	33.4
PTT/0.1 SWCNTs + 0.1 EG	53	232	46.9	184	46.8	32.1
PTT/0.05 SWCNTs	53	232	48.2	183	47.9	33.0
PTT/0.1 SWCNTs	53	231	48.4	180	48.7	33.2

T_g — glass transition temperature; T_m — melting temperature; T_c — crystallization temperature; ΔH_m, ΔH_c — enthalpy of melting and crystallization; ΔH_m^0 = 146 J/g, X_c — mass fraction of crystallinity determined from DSC.

Figure 4b depicts the heating curves of neat PTT and PTT/SWCNTs + EG hybrid nanocomposites. There is an endothermic melting peak on all of the heating scans. The values of melting parameters (T_m and ΔH_m) are summarized in Table 2. The melting temperatures and melting peak width are related to the lower thermal stability and the distribution of crystallites, respectively. The temperature of melting is virtually unchanged, regardless of hybrid nanofillers loading. A clear decrease in melting peak width is found in the nanocomposites with respect to neat PTT. In other words, the distribution of crystallites of PTT in PTT/SWCNTs + EG nanocomposites is narrower and lower than that of neat PTT. The values of ΔH_m for all nanocomposites are larger than that of PTT (45.8 J/g). However, they decrease with the increasing content of SWCNTs in hybrid system. This reveals that the degree of crystallinity of PTT increases with the addition of carbon nanoparticles. However, at the same time in the case of hybrid nanocomposites, and addition of CNT caused a slight decrease in X_c.

Thermal stability

The representative TGA and DTG curves only of neat PTT and PTT/SWCNTs + EG hybrid nanocomposites are shown in Fig. 5. The temperatures corresponding to 5 and 10 % of mass loss, activation energy of thermal decomposition and the maximum temperature of the mass loss rate for the whole series based on PTT are summarized in Table 3. Wang *et al.* [22], previously studied the thermal degradation of PTT with different molecular mass under argon, air, and nitrogen. They found three overlapping mass-loss stages in air atmosphere. However, in this case, PTT and its nanocomposites show two degradation steps in air and one in argon atmosphere, since the thermal stabilizer (Irganox 1010) has been applied. Moreover, similar observations were made previously in [4] for PTT reinforced with COOH functionalized multi-walled carbon nanotubes. The first step may correspond to the degradation of PTT chains into smaller part by the initial scissoring of chains' ends. During the second stage, these small fragments were oxidized into volatile products and the decomposition of some thermostable structures (such as aromatic structures) formed during former degradation processes has been observed. However, herein the presence of SWCNTs does not affect the degradation process of PTT. The temperature of maximum rate of mass loss (T_{DTG}, peak on DTG curve) was studied, to determine the thermal stability of the PTT/SWCNTs composites in

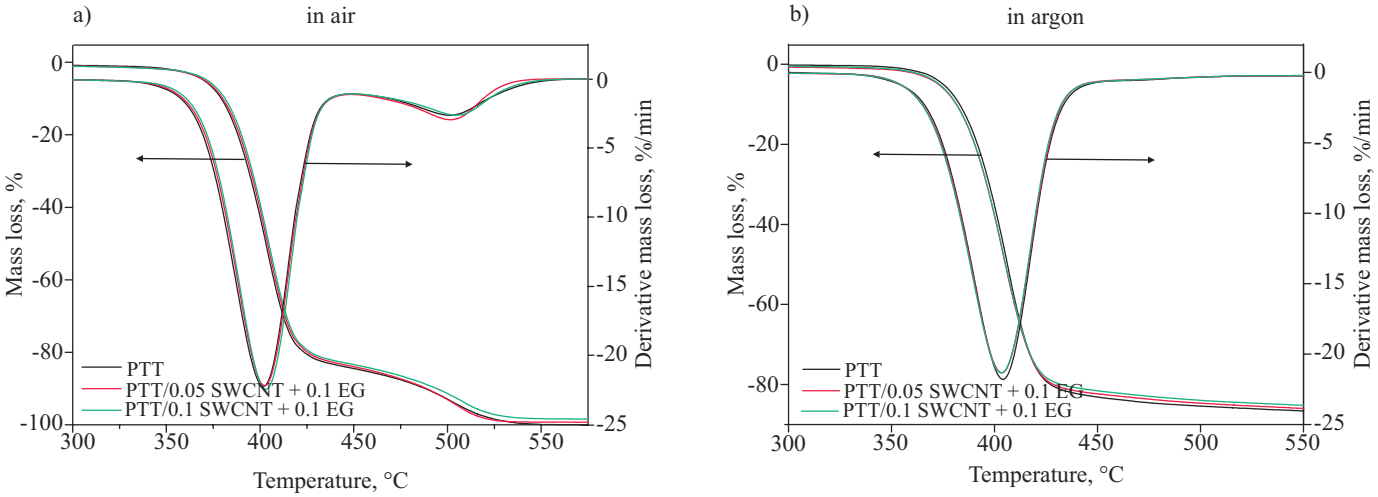

Fig. 5. Mass loss and derivative mass loss versus temperature for the PTT/SWCNTs + EG nanocomposites in: a) air, b) argon at a heating rate of 10 °C/min

detail. The temperature of maximum rate of mass loss T_{DTG1} of neat PTT in air and in argon were 401 and 404 °C, respectively. In the case of nanocomposites with highest concentration of SWCNTs the values of T_{DTG1} in air and argon were comparable to neat polymer.

Generally, graphene sheets exhibit very high thermal stability with only little mass loss up to 800 °C [23]. However, it was found that thermal stability, examined in argon atmosphere, of the nanocomposite with 0.1 wt % of EG and PTT matrix were comparable to one another.

T a b l e 3. Temperatures corresponding to 5 and 10 % mass loss, activation energy and the temperature at maximum of mass loss rate for the PTT/SWCNTs + EG nanocomposites obtained in air and argon atmosphere

Symbol	$T_{5\,\%}$ °C	$T_{10\,\%}$ °C	E_a kJ/mol	T_{DTG1} °C	T_{DTG2} °C
Measurement carried out in an oxidizing atmosphere					
PTT	370	379	318.39	401	501
PTT/0.1 EG	372	381	323.76	401	494
PTT/0.05 SWCNTs + 0.1 EG	371	380	327.86	402	502
PTT/0.1 SWCNTs + 0.1 EG	372	381	329.25	403	505
PTT/0.05 SWCNTs	372	382	323.87	404	508
PTT/0.1 SWCNTs	372	381	314.90	402	500
Measurement carried out in argon					
PTT	373	382	331.79	404	-
PTT/0.1 EG	373	382	343.47	403	-
PTT/0.05 SWCNTs + 0.1 EG	373	382	341.92	403	-
PTT/0.1 SWCNTs + 0.1 EG	373	382	339.15	403	-
PTT/0.1 SWCNTs	373	382	334.68	404	-

As it can be seen, similarly to nanocomposites with single nanofillers *i.e.* SWCNTs or EG, hybrid nanocomposites show similar thermal stability to pristine polymer and also temperatures corresponding to a maximum of mass loss (T_{DTG1}) didn't shifted to higher values with increasing content of nanofillers.

No effect on the thermal stability in an oxidizing and inert atmosphere for hybrid nanocomposites has been observed. Only in the case of activation energies of thermal decomposition a slight increase was observed. It can be concluded that the minimum energy that must be input to the system to cause the decomposition process is bigger in the case of nanocomposites than in neat PTT. No improvement of thermal stability of hybrid nanocomposites, with homogenous dispersion of nanofillers, might be caused by too small amount of both SWCNTs and graphene nanosheets to observe any effect.

Mechanical properties of PTT/SWCNTs + EG hybrid nanocomposites

Tensile properties were analysed also for the SWCNTs + EG reinforced PTT hybrid composites and the results are shown in Fig. 6. Here the stress is plotted against strain for all investigated samples. The average values and standard deviations (SD) for the Young's modulus (E), yield stress (elastic limit, σ_y), yield strain (ε_y), tensile strength (σ_b), and the strain at break (ductility, ε_b) are summarized in Table 4. Analysis of average values of modulus and their SD indicates that nanocomposites containing only SWCNTs or EG possess values of modulus lower or comparable to the neat PTT. For this composites high values of standard deviations for average values of σ_y and σ_b were observed. It can indicate that nanofillers are not homogenously dispersed in PTT matrix but also week interactions occur between the matrix and SWCNTs or EG. In our previous work on PTT based nanocomposites [4] up to 0.3 wt % loading of COOH functionalized multi-walled carbon nanotubes caused the increase of modulus and tensile stress at break. However, further addition of MWCNTs (0.4—0.5 wt %) low-

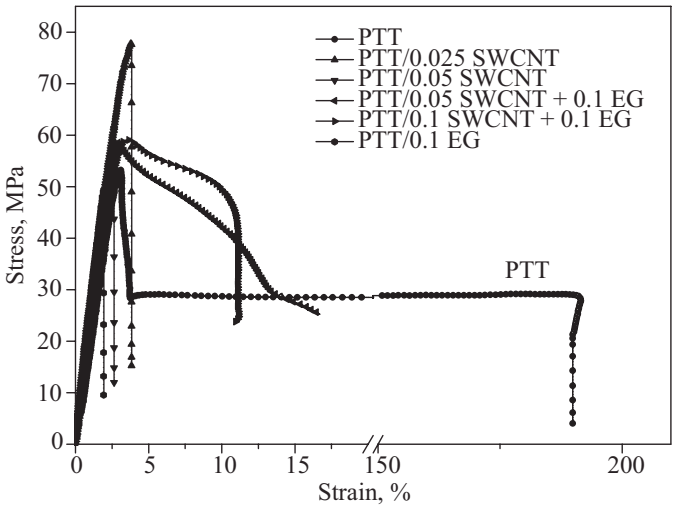

Fig. 6. Representative stress strain curves of PTT/SWCNTs + EG nanocomposites

0.1 SWCNT + 0.1 EG was added to PTT matrix. Perhaps with a higher CNT loading the homogenous dispersion of the tubes is getting to be more difficult to obtain and resulting in the existence of agglomerates. The probable cracks are originated at CNT agglomerates which behave as stress concentrators. Here, has been observed the dependence of the aspect ratio and the orientation of the single platelets crystallization at smaller strains, that does not appear for the unfilled sample. Similar effects would occur with CNT as reinforcing filler, if during the stress/strain measurements an orientation of the tubes took place. Such behavior could explain the increase of the stress especially at low strain, when compared to neat PTT. Moreover, the addition of both types of nanofillers induced crystallization resulting in decrease in ductility. However, since a combination of different types of nanofillers were applied, a clear statement seems to be difficult to provide and further investigations are necessary.

T a b l e 4. Tensile properties of PTT/SWCNTs + EG hybrid nanocomposites

Sample	E GPa	σ_y MPa	ε_y %	σ_b MPa	ε_b %
PTT	2.36 ± 0.05	50.2 ± 9.5	1.4 ± 0.3	28.6 ± 9.7	178 ± 32.4
PTT/0.025 SWCNTs	2.36 ± 0.12	68.9 ± 5.5	1.4 ± 0.1	68.9 ±5.6	3.8 ± 0.1
PTT/0.05 SWCNTs	2.38 ± 0.13	58.8 ± 9.2	1.1 ± 0.1	61.5 ± 5.3	2.6 ± 0.1
PTT/0.05 SWCNTs + 0.1 EG	2.44 ± 0.07	57.1 ± 1.3	1.2 ± 0.1	45.1 ± 3.4	16.3 ± 0.1
PTT/0.1 SWCNTs + 0.1 EG	2.29 ± 0.05	59.4 ± 3.2	1.3 ± 0.2	52.3 ± 2.3	11.2 ± 0.2
PTT/0.1 EG	2.37 ± 0.12	72.3 ± 4.5	1.5 ± 0.1	47.2 ± 6.7	1.9 ± 0.3

E — Young's modulus; σ_y — yield strength (elastic limit); ε_y — yield strain, σ_b, ε_b — stress and strain at break, respectively.

ered tensile strength and Young's modulus, but their values were still comparable or higher (modulus) to neat PTT. With an addition of EG of 0.1 wt % to nanotubes of 0.05 wt % into PTT matrix, a slight increase in the Young's modulus was observed. However, the increase of amount of CNT to 0.1 wt % in the mixture with EG causes the decrease in modulus, but at the very same time, this sample exhibits the lowest value of degree of crystallinity (Table 1). This may also have an impact on modulus and tensile strength. For both hybrid nanocomposites, the average values of σ_b are higher than for neat PTT. Taking into consideration the high value of standard deviation of σ_y for neat PTT and for hybrid composites, one can observe an increase of σ_y only for composite containing the highest loading of carbon nanofillers (0.1 SWCNT + 0.1 EG). Nanocomposite containing only EG also shows the increase of σ_y. Probable it was due to the dispersion state. In comparison to the neat PTT, the values of elongation at break for composites containing only CNT or EG showed a drastic decrease. Hybrid composites also showed a decrease of elongation at break, but this decrease is lower when compared with non-hybrid composites. It can be caused by an immobilization of the polymer chains and plays a significant role when a CNT network is formed. The results proved to be weaker when the system of

CONCLUSIONS

Hybrid SWCNTs/EG nanocomposites based on PTT with a total reinforcement of 0.2 wt % were synthesized by *in situ* polymerization and the effect of varying individual CNT/EG contents on morphology, mechanical properties and thermal stability were evaluated. This method enabled to control both the polymer architecture and the final structure of the composites. SEM and TEM confirmed good exfoliation of expanded graphite nanoplatelets along with well-distributed single-walled carbon nanotubes. The results obtained for the highest concentration of carbon nanofillers suggested, that the addition of hybrid system caused no appreciable change in the molecular masses. Moreover, T_m and X_c remained comparable to the neat PTT and nanocomposites with SWCNTs or EG. Despite a low concentration of carbon nanoparticles (total content below 0.2 wt %) an increase in the Young's modulus from 2.38 to 2.44 MPa with an addition of EG of 0.1 wt % to nanotubes of 0.05 wt % was observed. Additionally, in the case of activation energies of thermal decomposition a slight increase was observed. It can be concluded that a modest improvement of thermal stability and mechanical properties along with good distribution of nanoparticles that differ in shape, might

be caused by too small amount of both SWCNTs and EG to observe any effect. However, the presented study is only a part of a wider project on obtaining electrically conductive polymer hybrid nanocomposites with the total content of 1D+2D system as low as possible. In the further studies the research will be done in the terms of an influence of SWCNTs/EG addition on the electrical conductivity of PTT based nanocomposites.

ACKNOWLEDGMENTS

This work is the result of the research project no. 2013/11/N/ST8/00404 funded by National Science Centre. Sandra Paszkiewicz and Iwona Pawelec also thank for financial support from West Pomeranian University of Technology (Dean's grant for young scientists).

REFERENCES

[1] Houck M.M., Menold R.E.II, Huff R.A.: *Problems of Forensic Sciences* **2001**, *XLVI*, 217.

[2] Hsiao K.J., Lee S.P., Kong D.P., Chen F.L.: *Journal of Applied Polymer Science* **2006**, *102*, 945. http://dx.doi.org/10.1002/app.24053

[3] Wu G., Li H., Wu Y., Cuculo J.A.: *Polymer* **2002**, *43*, 4915. http://dx.doi.org/10.1016/S0032-3861(02)00306-3

[4] Szymczyk A., Rosłaniec Z., Zenker M. *et al*.: *eXPRESS Polymer Letters* **2011**, *5*, 977. http://dx.doi.org/10.3144/expresspolymlett.2011.96

[5] Hall L.J., Coluci V.R., Galvão D.S. *et al*.: *Science* **2008**, *320*, 504. http://dx.doi.org/10.1126/science.1149815

[6] Kim H., Miura Y., Macosko C.W.: *Chemistry of Materials* **2010**, *22*, 3441. http://dx.doi.org/ 10.1021/cm100477v

[7] El Achaby M., Arrakhiz F-A., Vaudreuil S. *et al.: Polymer Composites* **2012**, *33*, 733. http://dx.doi.org/10.1002/pc.22198

[8] Szymczyk A., Senderek E., Nastalczyk J., Roslaniec Z.: *European Polymer Journal* **2008**, *44*, 436. http://dx.doi.org/10.1016/j.eurpolymj.2007.11.005

[9] Szymczyk A.: *Journal of Applied Polymer Science* **2012**, *126*, 796. http://dx.doi.org/10.1002/app.36961

[10] Novoselov K.S., Geim A.K., Morozov S.V. *et al*.: *Science* **2004**, *306*, 666. http://dx.doi.org/10.1126/science.1102896

[11] Lee C., Wei X., Kysar J.W., Hone J.: *Science* **2008**, *321*, 385. http://dx.doi.org/10.1126/science.1157996

[12] Paszkiewicz S., Kwiatkowska M., Rosłaniec Z. *et al.: Polymer Composites* **2015**, http://dx.doi.org/10.1002/pc.23373

[13] Yang S., Lin W., Huang Y. *et al*.: *Carbon* **2011**, *49*, 793. http://dx.doi.org/10.1016/j.carbon.2010.10.014

[14] Pilawka R., Paszkiewicz S., Rosłaniec Z.: *Journal of Thermal Analysis and Calorimetry* **2014**, *115*, 451. http://dx.doi.org/10.1007/s10973-013-3239-4

[15] Paszkiewicz S., Nachman M., Szymczyk A. *et al*.: Polish Journal of Chemical Technology **2014**, *16* (*4*), 45. http://dx.doi.org/10.2478/pjct-2014-0068

[16] Paszkiewicz S., Szymczyk A., Špitalský Z. *et al*.: *Journal of Polymer Science, Part B: Polymer Physics* **2012**, *50*, 1645. http://dx.doi.org/10.1002/polb.23176

[17] Paszkiewicz S., Szymczyk A., Špitalský Z. *et al*.: *European Polymer Journal* **2014**, *50*, 69. http://dx.doi.org/10.1016/j.eurpolymj.2013.10.031

[18] Paszkiewicz S., Szymczyk A., Livanov K. *et al*: *eXPRESS Polymer Letters* **2015**, *9* (*6*), 509. http://dx.doi.org/10.3144/expresspolymlett.2015.49

[19] Hernandez J.J., Garcia-Gutiérrez M.C., Nogales A. *et al*.: *Composites Science and Technology* **2009**, *69*, 1867. http://dx.doi.org/10.1016/j.compscitech.2009.04.002

[20] Chuah H.H., Lin-Vien D., Soni U.: *Polymer* **2001**, *42*, 7137. http://dx.doi.org/10.1016/S0032-3861(01)00043-X

[21] Scheirs J., Long T.E.: „Modern Polyesters", Wiley & Sons Ltd. 2003, ISBN: 978-0-471-49856-8

[22] Wang X-S., Li X-G., Yan D.: *Polymer Degradation and Stability* **2000**, *69*, 361. http://dx.doi.org/10.1016/S0141-3910(00)00083-5

[23] Kim I.H., Jeong Y.G.: *Journal of Polymer Science, Part B: Polymer Physics* **2010**, *48* (*8*), 850. http://dx.doi.org/10.1002/polb.21956

Received 3 III 2015.